Optical-field-ionization effects on the propagation of an ultraintense laser pulse in high-*Z* gas jets

A. Zhidkov,[1] J. Koga,[2] T. Esirkepov,[2] T. Hosokai,[1] M. Uesaka,[1] and T. Tajima[2]
[1]*Nuclear Engineering Research Laboratory, Graduate School of Engineering, The University of Tokyo, 22-2 Shirane-shirakata, Tokai, Naka, Ibaraki 319-1188, Japan*
[2]*Advanced Photon Research Center, Japan Atomic Energy Research Institute, 8-1 Umemidai, Kizu-chou, Souraku-gun, Kyoto 619-0215, Japan*
(Received 24 June 2003; revised manuscript received 23 February 2004; published 9 June 2004)

Interaction of an ultraintense, $a_0 \gg 1$, laser pulse with an underdense Ar plasma is analyzed via a two-dimensional particle-in-cell simulation which self-consistently includes optical-field ionization. In spite of rapid growth of ion charge Z and, hence, electron density at the laser front, relativistic self-focusing is shown to persist owing to a reduction of the expected plasma defocusing resulting from the weak radial dependence of the ion charge on laser intensity (even for $Z/\gamma > 1$ where γ is the electron relativistic factor).

DOI: 10.1103/PhysRevE.69.066408 PACS number(s): 52.38.−r

Plasma ionization plays an important role in the interaction of ultraintense, short laser pulses with gas jets [1–7]. When the electric field strength of a laser pulse, $a_0 = eE/mc\omega = 8.5 \times 10^{-10} \lambda\ (\mu\mathrm{m})\ [I\ (\mathrm{W/cm^2})]^{1/2}$, exceeds the atomic field strength, $a_A = E_A/mc\omega = me^6/ch^4\omega = 3.05 \times 10^{14}/\omega$, the plasma electron density increases rapidly at the front of the laser pulse due to optical field ionization (OFI). At relatively low laser intensity, this rapid change of electron density can be the source of various nonlinear processes such as self-defocusing, laser frequency up-shift, ring formation, and others. For a typical $a_0 < 1$ laser pulse, the electron density reaches its maximum, and the plasma permittivity, $\varepsilon = 1 - \omega_{\mathrm{pl}}^2/\omega^2$ where ω_{pl} is the plasma frequency, reaches its minimum, along the pulse axis. This results in the pulse self-diffraction [2] with a concomitant intensity decrease. These effects have been studied theoretically and experimentally, mostly for low-Z gases and weakly relativistic intensities [2–4].

For a high-Z gas irradiated by a laser pulse, the maximal ion charge can be estimated from a simplified equation by setting $\nu_{\mathrm{OFI}}(I_Z)\tau = 1$, where

$$\nu_{\mathrm{OFI}} = 4\omega_{\mathrm{A}}(I_Z/\mathrm{Ry})^{5/2}(a_{\mathrm{A}}/a_0)\exp[-2(I_Z/\mathrm{Ry})^{3/2}a_{\mathrm{A}}/(3a_0)] \tag{1}$$

is the optical-field-ionization probability rate [8,4–7], I_Z is the ionization potential,

$$I_Z = Z^2\mathrm{Ry}/n_{\mathrm{eff}}^2, \tag{2}$$

τ is the pulse duration, $\omega_A = 4.1 \times 10^{16}\ \mathrm{s}^{-1}$ is the atomic frequency, Ry = 13.6 eV, and n_{eff} is the effective state number. After a simple calculation, one can find that

$$I_z \sim \mathrm{Ry}\{1.5\ a_0/a_{\mathrm{A}}[A + \ln(4\omega_{\mathrm{A}}\tau a_{\mathrm{A}}/a_0)]\}^{2/3}, \tag{3}$$

where $A = 2.5\ \ln(I_Z/\mathrm{Ry})[\sim 10, \text{for } I_Z \sim (0.5-1)\mathrm{keV}$; A is approximately constant at reasonable $a_0 < 100$. For Ar atoms and $a_0 > 2$ this equation gives $Z \sim 10$ so that the electron density rises ten times at the pulse front. Due to additional axial compression produced by the ponderomotive force, the electron density can approach critical density $N_{\mathrm{cr}} = m\omega^2/4\pi e^2$. Such a strong change in the plasma density affects the laser pulse propagation. According to the simplified theory [1], the plasma permittivity increases as $\varepsilon = 1 - \omega_{\mathrm{pl}}^2/\omega^2\gamma = 1 - N_{\mathrm{e}}/\langle\gamma\rangle N_{\mathrm{cr}}$, where N_{e} is the electron density and $\langle\gamma\rangle$ is the effective relativistic factor of the plasma electrons. According to Ref. [1], $\langle\gamma\rangle = (1 + a_0^2/2)^{1/2}$ and the permittivity may have a maximum on axis if a_0 increases faster than the ion charge, Z. At first sight, the effect of OFI, which results in diffraction or in self-focusing, simply depends on the competition between the radial electron density gradient at the front of the laser pulse (which leads to diffraction) and the relativistic factor (which determines the self-focusing strength). These arguments assume the laser field is greater than the ion charge, $Z/a_0 \ll 1$. For a high-Z gas this happens only if ultrarelativistic laser pulses with $a \gg 10$ are employed. However, self-focusing of laser pulses can occur even for $Z/a_0 > 1$. To show this we consider the dependence of the mean ion charge on the laser field. According to Eqs. (2) and (3), the ion charge is equal to $Z = Ba_0^{1/3}$, where B is large but nearly constant. Hence, inside the laser pulse, for $a \gg 1$ the permittivity is $\varepsilon = 1 - BN_0/a_0^{2/3}$, $N_0 = 2^{1/2}N_{\mathrm{i0}}/N_{\mathrm{cr}}$, where N_{i0} is the initial ion density, and has a maximum along the pulse axis and, therefore, even a small diffraction loss of energy of the laser pulse can maintain its strong self-focusing. In the present paper, we investigate numerically the interaction of relativistically intense laser pulses with an underdense high-Z plasma of Ar with $Z/a_0 > 1$.

To study the propagation of the intense laser pulse in an Ar gas jet, we apply a fully relativistic two-dimensional (2D) particle-in-cell (PIC) simulation with the "moving window" technique with mobile Ar ions [9]. A 2D simulation is relevant as a form of the paraxial equation [10]. The plasma length is infinite with a steep density gradient. We use 36 particles per cell in a $160 \times 120\ \mu\mathrm{m}^2 (2800 \times 2048$ cells) window, which moves at the speed of light. A $\lambda = 0.8\ \mu$m linearly polarized laser pulse with a full width at half maximum duration of 20 fs and an intensity of $I = 10^{19-21}\ \mathrm{W/cm^2}$ is focused to a 16 μm spot (which corresponds in 3D to a Rayleigh length of 725 μm). (The difference between the calculated absorbed laser energy and total plasma energy is less than 1%. The numerical error in the

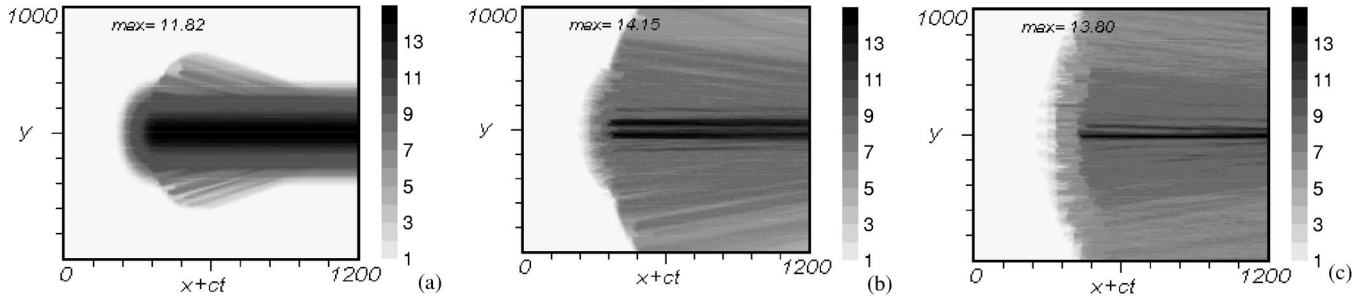

FIG. 1. Temporal and spatial evolution of ion charges in an Ar gas jet with $N_0=10^{19}$ cm^{-3} irradiated by a 20 fs, *s*-polarized laser pulse with $I=10^{20}$ W/cm^2: (a) $\omega t=500$, (b) 1100, (c) 1900. The maximum value given in the figure is the maximum ion charge. Coordinates are given in $\omega/c:x$ (μm)$=0.127x$ (normalized); t(fs)$=0.42t$ (normalized).

group velocity is smaller than the velocity deviation from the speed of light.) Initially the plasma is singly ionized. In the beginning, the laser pulse propagates 50 μm in very low density plasma, $N_{e0}=10^{13}$ cm^{-3}; then it crosses the steep plasma edge with density, $N_{e0}=10^{19}$ cm^{-3} (The laser intensity exceeds the critical power for relativistic self-focusing $P_{cr}=17(\omega/\omega_{pl})^2$ [GW] at $Z=1$ in 3D geometry.) We assume no clusters in the jet due to elimination by the laser prepulse.

In the method used to include plasma ionization, the plasma charge is modified by varying the number of particles. The charge of the electron particles is fixed so that if all electron particles were involved in the calculation, the plasma density would be equal to that of the fully ionized plasma [5,6]. At the onset of the calculation, there are n_{PIC}

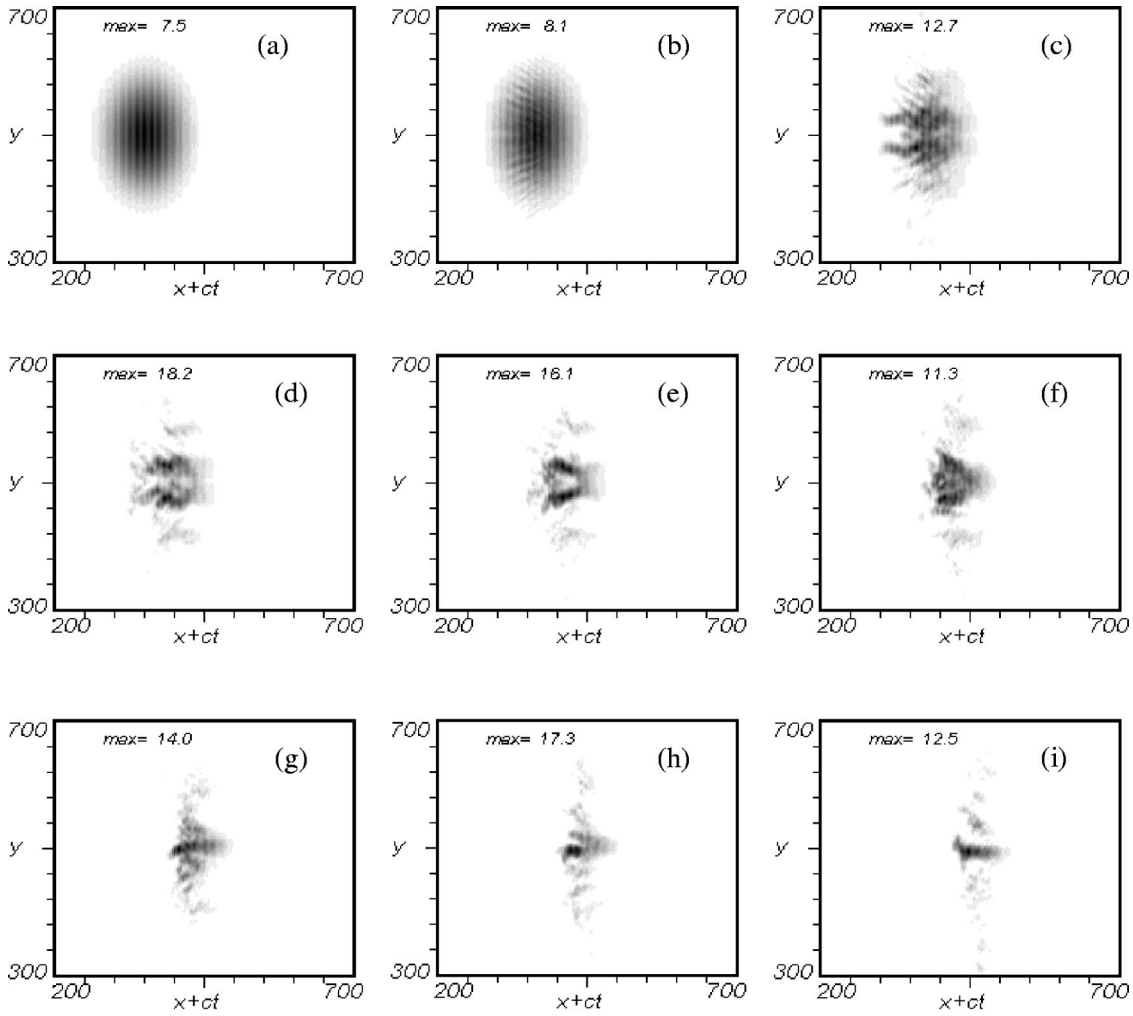

FIG. 2. Temporal and spatial evolution of normalized laser intensity, $E_z^2+H_x^2+H_y^2$, in an Ar gas jet for a 20 fs, *s*-polarized laser pulse with $I=10^{20}$ W/cm^2. (a)$\omega t=0$, (b) 500 (c) 850, (d) 1100, (e) 1350, (f) 1450, (g) 1600, (h) 1700, (i) 1900. The laser pulse is propagating from the right to the left. The maximal value in each figure refers to maximal normalized intensity in the window.

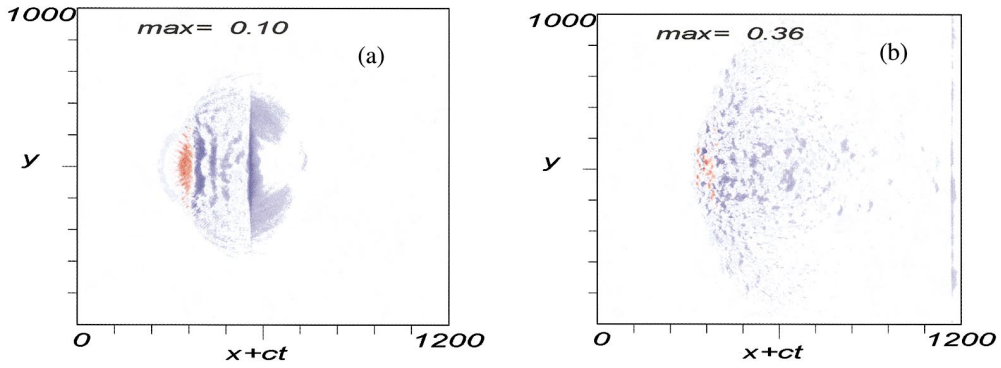

FIG. 3. (Color) The x component of the plasma electric field, (a) $\omega t=500$, (b) 850. The maximal value in each figure refers to a maximal positive E_x in $e/mc\omega$ units.

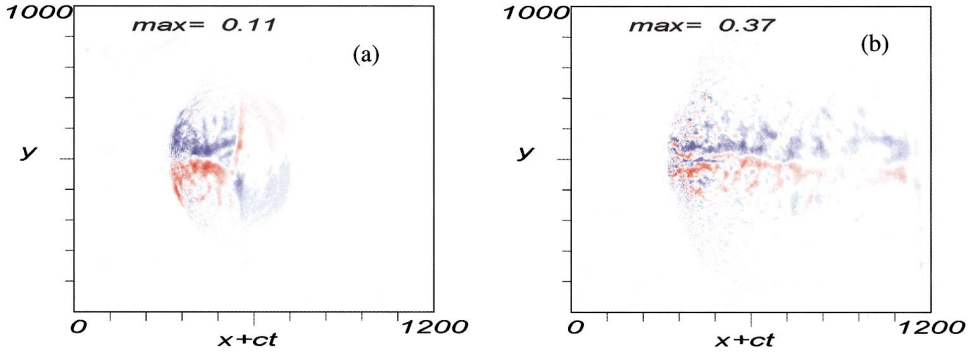

FIG. 4. (Color) Z component of the plasma magnetic field, (a) $\omega t=500$, (b) 850. The maximal value in each figure refers to a maximal positive H_Z in $e/mc\omega$ units.

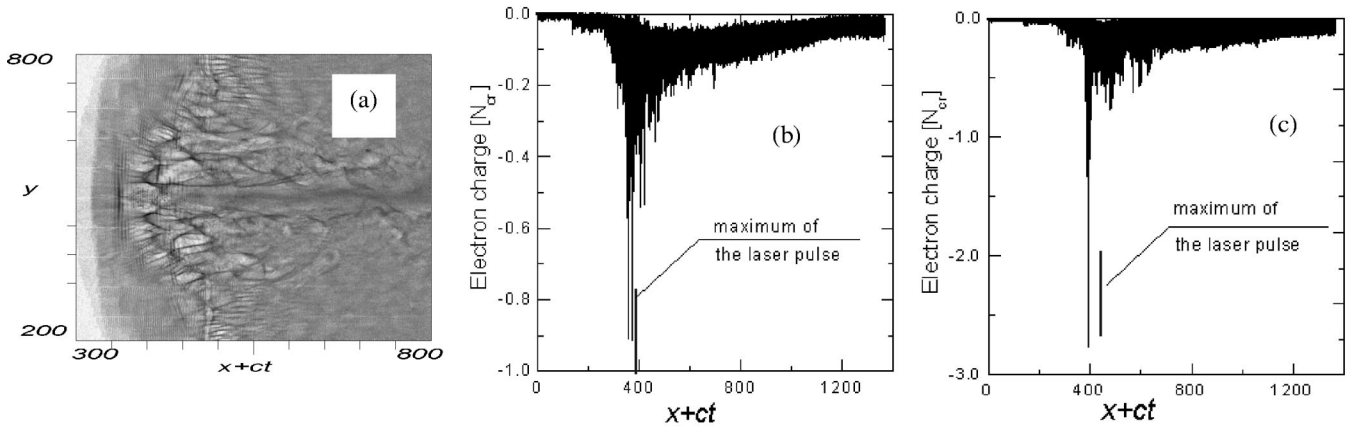

FIG. 5. Electron charge distribution in the plasma at $\omega t=1350$: (a) 2D plot, N_{max} is in units of N_{cr}; (b) 1D plot along the laser axis at $I=10^{20}$ W/cm^2; and (c) $I=10^{20}$ W/cm^2.

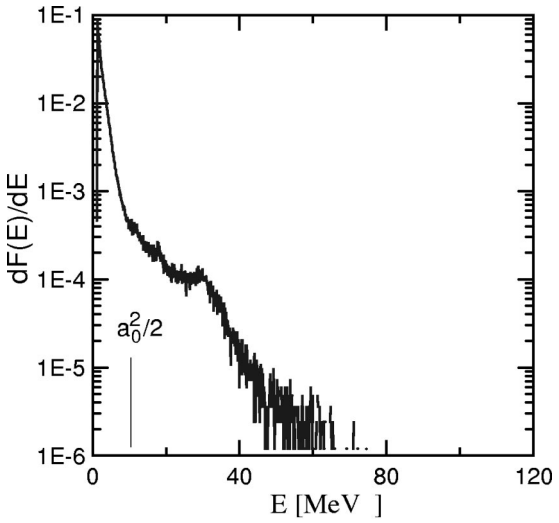

FIG. 6. Electron energy distribution at $\omega t = 1900$.

electron particles involved in the PIC calculation while $n_{\mathrm{PIC}}(Z_{\mathrm{A}}-1)$ electron particles (n_{PIC} is an integer, Z_{A} is the nuclear charge, $Z_{\mathrm{A}}=18$ for Ar) move with an ion. We calculate the equation $dZ/dt=\nu_{\mathrm{OFI}}[Z(t)]$ for every ion. (This equation can be easily derived from the balance equation for electron charge [5].) Discrete, real ionization potentials are used for the Ar ions. When the charge Z of an ion particle (not the total charge) exceeds an integer, an additional n_{PIC} electron particle becomes involved in the field and current calculation. To conserve energy we define an ionization-loss current $\boldsymbol{j}_{\mathrm{A}}$ [5]; Ohmic heating, $U_{\mathrm{A}}=\boldsymbol{j}_{\mathrm{A}}\boldsymbol{E}$, produced by this current provides a laser energy loss equal to the plasma ionization. Net charge conservation is invoked using the condition $\mathrm{div}\boldsymbol{j}_{\mathrm{A}}=0$, which is always true for an *s*-polarized 2D pulse simulation. We neglect the Kerr self-focusing (see Ref. [7]). In the absence of clusters, the nonlinear third-order term in the polarization responsible for the Kerr effect can be estimated as follows: $\boldsymbol{P}_3 \sim d\boldsymbol{E}\langle d\boldsymbol{E}\rangle^2/\boldsymbol{\Omega}_{\mathrm{R}}^2=\chi_3 E^2\boldsymbol{E}$, where $\boldsymbol{d}$ is the dipole moment, $\boldsymbol{E}$ is the laser field, $\boldsymbol{\Omega}_R=[(h\omega_{\mathrm{R}})^2+(\boldsymbol{dE})^2]^{1/2}$ with $h\omega_{\mathrm{R}}$ being the energy of the closest level. For transitions with $\Delta n=0$, ω_{R} increases in proportion with the ion charge, $\sim Z$; the dipole moment decreases as Z^{-1}. For $a_0>1$ the term $\boldsymbol{d}E$ becomes dominant and the nonlinear term in $\chi_3 E^2$ saturates and decreases as $a_0^{-2/3}$ (we assume $Z\sim a_0^{1/3}$). For transitions with $\Delta n=1$ ($\omega_{\mathrm{R}}\sim Z^2$ and $\boldsymbol{\Omega}_{\mathrm{R}}\sim h\omega_{\mathrm{R}}$), one can obtain that $\chi_3 E^2 \sim a_0^2/Z^6$ is constant, however, $\boldsymbol{P}_3$ itself decreases as Z^{-1} and finally the nonlinear term decreases as Z^{-16}. This allows us to include only plasma effects in the present calculation.

The temporal evolution of the average ion charge in an Ar plasma irradiated by a short laser pulse with $I=10^{20}$ W/cm^2($a_0=6.8$) is shown in Fig. 1. Note that even in the low density plasma region, the ion charge Z exceeds 10, Ar^{+11} and Ar^{+12} are the most abundant ions. Charge traces resulting from the strong diffraction of the laser pulse entering the steep plasma edge clearly can be seen. With time Ar^{+14} and Ar^{+15} ions appear along the center of the laser axis due to laser relativistic self-focusing. At the periphery of the laser pulse, Ar^{+9} and Ar^{+10} ions are most abundant. The electron density smoothly rises in the area, not only because of the cube-root dependence of the ionic charge on the laser field, $Z\sim a_0^{1/3}$, but also due to strong diffraction of the pulse. Since there is no efficient recombination during the duration of the simulation window and ions are too heavy to move fast, the structure of the traces are striated displaying the structure of the laser pulse electric field. For laser intensities $I=10^{19}(a_0=2.15)$ and $I=10^{21}$ W/cm^2($a_0=21.5$) the spatial distribution of the ion charges is qualitatively similar to that presented in Fig. 1, though numerically different: the maximum values of the ionic charge along the laser axis are $Z_{\mathrm{max}}=12$ and $Z_{\mathrm{max}}=16$, respectively.

Figure 2 shows the temporal evolution of the normalized laser intensity with $I=10^{20}$ W/cm^2. For nonrelativistic laser intensity, $a_0<1$, the laser pulse would rapidly diffract from a combination of the radial electron density gradient (i.e., plasma defocusing from the OFI generated plasma), reduced relativistic self-focusing, and vacuum diffraction. According to the linear ray equation in linear theory, the angle between a light trajectory and the propagation axis changes as $\partial\theta/\partial x=-(2N_{\mathrm{cr}})^{-1}\partial N_{\mathrm{e}}/\partial r$ [10,11] so that the light totally diffracts ($\theta=\pi/2$) at $L\sim \pi N_{\mathrm{cr}}\, d/N_{\mathrm{e}}$ where d is of the order of the laser spot size. Since the electron density is close to the critical density in the Ar gas jet, the diffraction length of the laser pulse can be much shorter than its Rayleigh length. For relativistic intensity, strong self-focusing along with strong diffraction is clearly seen. However in contrast to self-focusing in a uniform plasma, the ring formation similar to that observed in experiments of Ref. [3] is found. This ring has a diameter of about 6 μm with a maximal laser intensity as much as 2.5 times the initial. The ring oscillates as the pulse propagates through the plasma [see Figs. 2(d)–2(g)]. Within our understanding, this instability is related to the hosing of the self-focused laser pulse [12,13]. To estimate the effect of diffraction on the pulse propagation we calculate the pulse energy change in a strip with the transverse size of about 20 μm which initially contains 99% of the laser energy. The depletion length L_{D} of the self-focused laser pulse (70% of energy lost) is 0.4 mm for the laser intensity $I=10^{20}$ W/cm^2. We observe that the depletion length increases with laser intensity and is about 0.6 mm for $I=10^{21}$ W/cm^2 ($L_{\mathrm{D}}=0.15$ mm for $I=10^{19}$ W/cm^2). We attribute this effect to the reduced diffraction loss of the laser pulse. As the laser intensity increases, a smaller fraction of the pulse energy is necessary to form a smooth density distribution in the vicinity of the self-focused laser pulse because the ion charge saturates and more laser energy can continue to be relativistically focused forward.

The plasma electric and magnetic field distributions in an Ar plasma irradiated by a $I=10^{20}$ W/cm^2 laser pulse are given in Fig. 3 and Fig. 4, respectively. Initially, the x component of the plasma electric field [Fig. 3(a)] has a wake-field structure. Wave breaking rapidly appears at $E_{\mathrm{x}}=0.3mc\omega/e$ [Fig. 3(b)] which is much smaller than the relativistic wave-breaking threshold. For lower and higher laser intensity, the field distribution is qualitatively the same.

In the magnetic field distribution one can see a magnetic channel with a diameter equal to that of the self-focused laser ring. Assuming that this current is produced by relativistic electrons we estimate the electron density in the current as

$N_{ech}=N_{cr}c/(\omega d)$ where d is the channel diameter. This density is considerably lower than the critical density.

The spatial distribution of the electron density after the laser pulse has propagated 0.15 mm into the plasma is shown in Fig. 5(a). A strong electron bunch 8 μm in size in the longitudinal and 30 μm in size in the transverse direction is formed via ponderomotive acceleration. The maximal density in the bunch is $0.8N_{cr}$ [though the average density is $0.2N_{cr}$, see Fig. 5(b)] at $I=10^{20}$ W/cm^2. For higher intensity, N_{max} exceeds the critical density and the average density in the bunch is half of the critical density, as seen in Fig. 5(c). Transverse motion of electrons in the bunch limits its average density. The mean velocity of electrons in the bunch is close to $v=c(1-4/a_0^4)$ which corresponds to the ponderomotive potential of the laser pulse. Electrons in the bunch move faster than the laser pulse as seen in Fig. 2(e) where the group velocity is 4–6 % less than the light speed. The energy distribution of the electrons is shown in Fig. 6. Since electrons in such an electron bunch are strongly relativistic, it could serve as a relativistic mirror for a counter-propagating long-wavelength laser pulse [14].

In conclusion, we have observed the self-focusing of a relativistically intense laser pulse in a dense Ar gas jet under the condition when density growth due to optical-field ionization cannot be totally compensated by relativistic effects such that $Z/\gamma>1$. We have demonstrated that this self-focusing is maintained by small diffraction loss of the laser pulse energy. Because of the slow dependence of the maximum ionic charge on the laser field $\sim a_0^{1/3}$, the transverse derivative of the electron density is much smaller than that of the laser field, $N_e^{-1}dN_e/dr \ll a_0^{-1}da_0/dr$, and Z/γ has a minimum along the laser axis which maintains self-focusing. Due to ponderomotive acceleration a high density [$\langle N_e\rangle \sim (0.3-0.5)N_{cr}$] electron bunch is formed in front of the laser pulse. The group velocity of the laser pulse is not considerably reduced by this effect.

This work was partially supported by National Institute of Radiological Sciences, Japan.

[1] W. P. Leemans, C. E. Claton, W. B. Mori, K. A. Marsh, P. K. Kaw, A. Dyson, C. Joshi, and J. M. Wallace, Phys. Rev. A **46**, 1091 (1992); P. Sprangle, J. R. Penano, and B. Hafizi, Phys. Rev. E **66**, 046418 (2002); D. L. Bruhwiler, D. A. Dimitrov, John R. Cary, E. Esarey, W. Leemans, and R. E. Giacone, Phys. Plasmas **10**, 2022 (2003); B. Hafizi, P. Sprangle, J. R. Peñano, and D. F. Gordon, Phys. Rev. E **67**, 056407 (2003).

[2] C. S. Liu and V. K. Tripathi, Phys. Plasmas **7**, 4360 (2000).

[3] P. Chessa, E. De Wispelaere, F. Dorchies, V. Malka, J. R. Marques, and G. Hamoniaux, Phys. Rev. Lett. **82**, 552 (1999).

[4] N. E. Andreev, M. V. Chegotov, and A. A. Pogosova, JETP **96**, 885 (2003).

[5] A. Zhidkov and A. Sasaki, Phys. Rev. E **59**, 7085 (1999); Phys. Plasmas **7**, 1341 (2000).

[6] S. Kato and Y. Kishimoto, and J. Koga, Phys. Plasmas **5**, 292 (1998).

[7] P. Sprangle, E. Esarey, and J. Krall, Phys. Rev. E **54**, 4211 (1996).

[8] L. V. Keldish, JETP Lett. **20**, 1307 (1965); L. Landau and E. Lifshitz, *Quantum Mechanics* (Pergamon, Oxford, 1975); A. M. Peremolov, V. S. Popov, and V. Terent'ev, JETP Lett. **23**, 924 (1966).

[9] R. G. Hemker, K. C. Tzeng, W. B. Mori, C. E. Clayton, and T. Katsouleas, Phys. Rev. E **57**, 5920 (1998); B. J. Duda, R. G. Hemker, K. C. Tzeng, and W. B. Mori, Phys. Rev. Lett. **83**, 1978 (1999).

[10] M. Born and E. Wolf, in *Principles of Optics*, 7th ed., (Cambridge University Press, Cambrdige, England, 1999).

[11] L. Landau and E. Lifshitz, *The Electrodynamics of Continuous Media* (Pergamon Press, New York, 1961).

[12] Z. Najmudin, K. Krushelnick, M. Tatarakis, E. L. Clark, C. N. Danson, V. Malka, D. Neely, M. I. K. Santala, and A. E. Dangor, Phys. Plasmas **10**, 438 (2003).

[13] W. B. Mori, T. Katsouleas, J. M. Dawson, and C. H. Lai, Phys. Rev. Lett. **74**, 542 (1995); R. L. Savage, C. Joshi, and W. B. Mori, *ibid.* **68**, 946 (1992); W. B. Mori, Phys. Rev. A **44**, 5118 (1991); N. M. Naumova, J. Koga, K. Nakajima, T. Zh. Esirkepov, S. V. Bulanov, and F. Pegoraro, Phys. Plasmas **8**, 4149 (2001); S. V. Bulanov *et al.*, Phys. Fluids B **4**, 1935 (1992).

[14] S. V. Bulanov, T. Esirkepov, and T. Tajima, Phys. Rev. Lett. **91**, 085001 (2003).